JOURNAL OF Applied Polymer SCIENCE

Mechanical and Thermal Properties of Compatibilized Polypropylene Reinforced by Woven Doum

Mustapha Malha,[1] Souad Nekhlaoui,[1] Hamid Essabir,[2,3] Khalid Benmoussa,[2] Mohammed-Ouadi Bensalah,[1] Fatima-Ezzahra Arrakhiz,[2] Rachid Bouhfid,[2] Abouelkacem Qaiss[2]

[1]Faculty of Science, Mohammed V-Agdal University, Laboratory of Mechanic and Materials, Rabat, Morocco

[2]Moroccan Foundation for Advanced Science, Innovation and Research (MASCIR), Institute of Nanomaterials and Nanotechnology, Laboratory of Polymer Processing, Rabat, Morocco

[3]National School of Applied Sciences, Ibn Zohr University, Laboratory of Mechanics, Processes, Energy and Environment (LMPEE), Agadir, Morocco

Correspondence to: A. Qaiss (E-mail: a.qaiss@mascir.com).

ABSTRACT: In this work, the development and the mechanical characterization of a doum textile composite based on a polypropylene matrix were carried out. Mechanical and rheological tests were effectuated, to illustrate the effect of woven fibers on the mechanical and viscoelastic properties at 0°, 15°, 30°, and 45° directions. The woven fibers were treated and the matrix was melted to a coupling agent to assure compatibility between the fibers and the polymer. The composites with long fiber are generally used as film and the main properties is the tensile. In this study, our goal was to improve the tensile properties. Results have shown that tensile properties exhibited a significant increase when compared to the polypropylene. However, it was observed that the stress direction has no influence on the thermal properties of the composite. Also, this article evaluates models that predict the stiffness of the composites at different stress directions to be compared to the experiments. © 2013 Wiley Periodicals, Inc. J. Appl. Polym. Sci. 000: 000–000, 2013

KEYWORDS: composites; fibers; textiles

Received 26 February 2013; accepted 3 June 2013; Published online 00 Month 2013
DOI: 10.1002/app.39619

INTRODUCTION

Nowadays, the interest on the increase of environmental awareness has impacted the material manufacturing, general products made by non-renewable resources required substantial amount of energy for productions that would excessively generate carbon dioxide.[1] Thus, the introduction of natural fillers from renewable resources for structural composites can be benefits to the environment[2] with respect to their bio-degradability, costs and natural availability.[3] Many studies on plant fillers (fiber and particle) as alfa,[4] coir,[5] sugarcane bagasse,[6] doum,[7] almond shells,[8] and argan shells[9] as reinforcement for thermoplastic or thermoset polymers have been conducted. The advantages of the natural fibers are their abundance, low cost, high specific modulus, and lightweight compared to synthetic fibers.[10,11] However, one of the main limitations of using fibers in high strength composite applications is their poor adhesion properties with the polymeric matrix.[2,12] Additionally, natural fibers cannot resist to high temperature,[1,13] which limits the curing or extrusion during composite manufacturing. All these problems can be overcome by adding coupling agent as silane[5,14] or maleic anhydride (MA)[15] into the composites or by treating fibers with suitable chemicals to decrease the hydrophilic hydroxyl groups on the surface of fibers,[16] which improve the hydrophobic characteristics and facilitate a better bonding with the matrix.[16] The alkali treatment is the standard chemical modifications of the surface of the fibers by removing the amorphous materials.[16] On the other hand, the maleic anhydride grafted styrene-(ethylene-butene)-styrene (SEBS) or polypropylene (PP) is used with polypropylene or high density polyethylene as coupling agent due to its compatible structure with olefinic block.[17] The use of SEBS which has rubber character, improve the ductility of polymeric matrix reinforced with fibers instead of MA-*g*-PP.[8]

In general, the long and short fibers improve the properties of materials. The short fibers are used in the material processed using the extruder and injection machine,[7] but in the case of long fiber it is possible to fabric the materials as film,[18] such as textile composite; these composites presents several advantages when it provides inherent reinforcement in multiple directions[19] especially when they are suitable for polymer reinforcement. For several years, these two dimensional structures have been used in maritime craft, air craft, high performance automobiles, and civil infrastructure.[20] And the characterization of textile composites got an important place in structural design.[21] However,

Applied Polymer SCIENCE

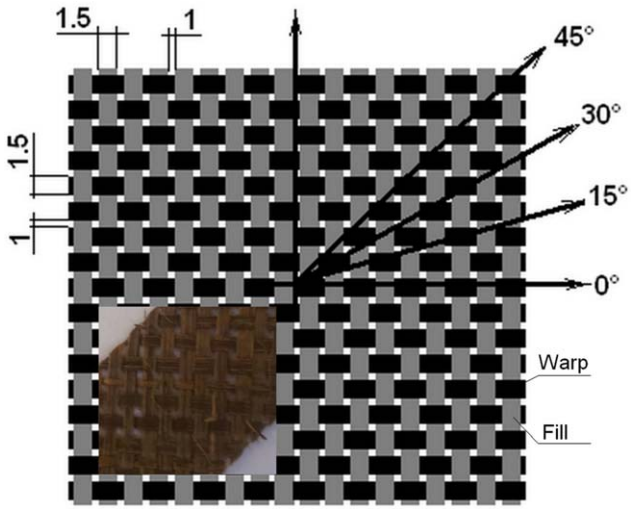

Figure 1. Structure of woven Doum fiber. [Color figure can be viewed in the online issue, which is available at wileyonlinelibrary.com.]

due to the anisotropic and inhomogeneous character of materials, parameters controlling mechanical properties are numerous, such as fiber architecture, fiber properties, and matrix properties.[20,22]

The doum palm (*Chamaerops humilis*) belongs to the family of monocots, such as grasses, Musaceae (banana). The used fibers are extracted from the petioles doum palm. The sheet is composed of petiole attached to the trunk which grows on the leaflet. Fiber length obtained depends on the type of tree, shape, and age. In this work, the doum fiber has been selected in this study as reinforcement in woven material reinforcing a polypropylene matrix not only because of their good mechanical properties, but also in a context of valorizing abundant and unexploited Moroccan fibers.[7,23] A coupling agent was added to the matrix at 8 wt % to improve compatibility of the resulting composite, namely a styrene-(ethylene-butene)-styrene triblock copolymer grafted with maleic anhydride (SEBS-*g*-MA). It is also important to note that fibers were alkali treated before incorporating in the matrix .The samples for mechanical tests were prepared in rectangular shape and following four directions (0°), (15°), (30°), and (45°). A basic measure of the density of the textile composite and the woven fibers reveals that the weight percentage of fibers is 42% and the matrix is 58% (PP-SEBS-*g*-MA).

MATERIALS AND EXPERIMENTAL SECTION

Materials

PP was used to prepare a reinforced composite (ExxonMobil chemical, a density of 0.9 g/cm^3, and melting temperature of 165°C). Styrene-(ethylene-butene)-styrene three block copolymer grafted with maleic anhydride (SEBS-*g*-MA) was supplied by Shell (Kraton FG-1901X) containing 1.4 to 2 wt % MA. In order to take more advantage of local crops raw, doum palm (*C. humilis*) fibers were used as reinforcement in PP matrix and treated before further use. The chemical products used for treatment are NaOH (sodium hydroxide, Sigma Aldrich, 98%), CH_3COOH (acetic acid, Riedel- de haën, 99–100%).

Preparation of Woven Fabrics of Doum Palm

Woven fabrics usually consist of two interlacing yarns: fill and warp. In the present study, the angle between the fill and warp yarns is 90°, as shown in Figure 1. These woven fabrics were not commercially available and were made with a homemade system, as shown in Figure 2(a,b). Where Figure 2(a) shows how filler are extracted and Figure 2(b) shows the system used to woven them. The fabric utilized was of balanced plain woven and there were one warp and one fill yarn per 4 mm (around 200 yarns by warp and fill). Width of each warp and fill was 1.5 mm while the gap between the adjacent one was 1 mm, approximately as illustrated in Figure 1 and the thickness of starting fabric was around 400 μm.

Chemical Treatment of Woven Fabrics and PP Modification Procedure

The woven doum fibers were first kept for 48 hours in a 1.6 mol/L sodium hydroxide aqueous solution,[4] then treated with acetic acid (100 mL) to neutralize the remaining hydroxide.[24] These fibers were finally air-dried for 24 h before further use. It was shown the morphology of raw fibers [Figure 3(a,a')] and alkali treated fibers [Figure 3(b,b')]. The Alkali treatment removes a certain amount of lignin, waxes, and oils covering the external surface of fibers which could limit the adhesion with the polymeric matrix.[25] Many research studies have been

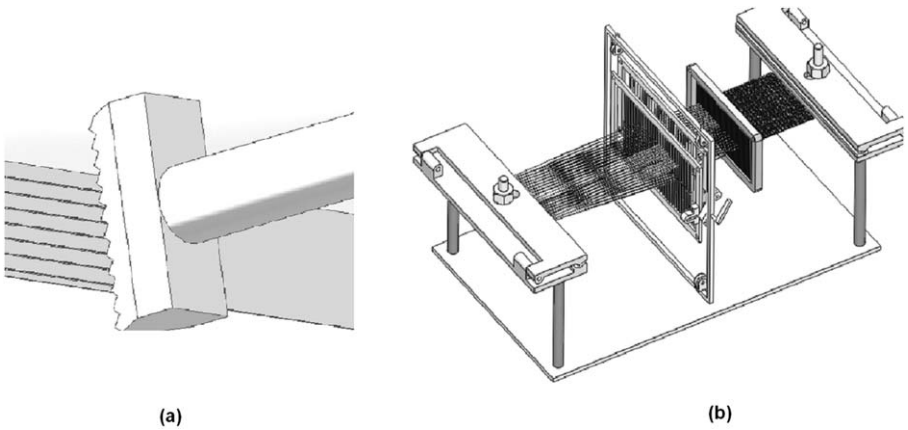

Figure 2. The schematic illustration of (a); multi cutter; (b) a homemade textile machine.

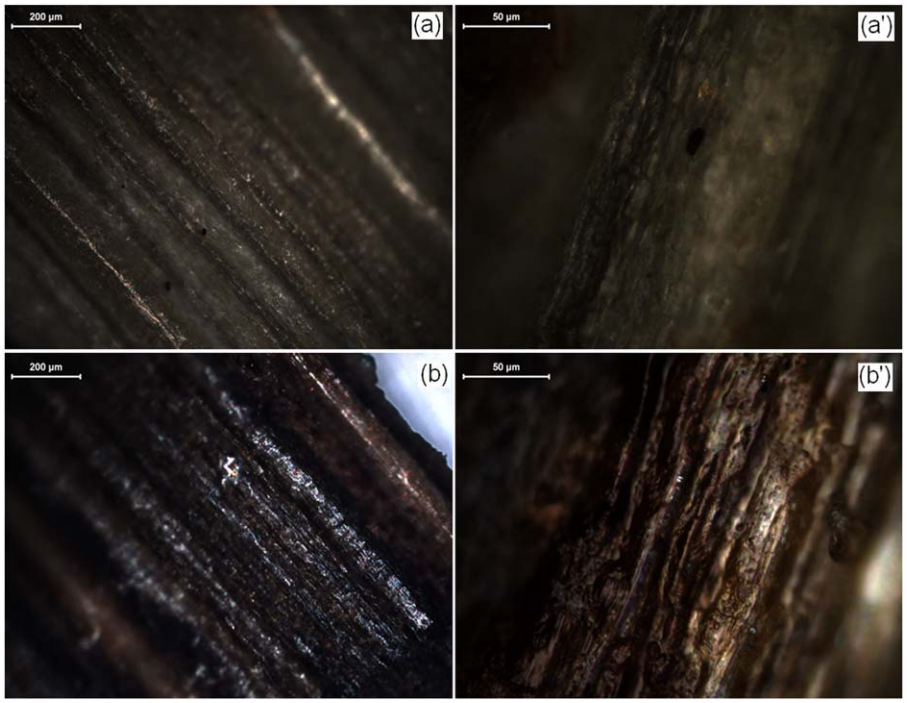

Figure 3. Morphology of Doum fibers: (a) raw fibers at 10× magnification; (a′) raw fibers at 50× magnification; (b) alkali Doum fibers at 10× magnification; (b′) alkali doum fibers at 50× magnification. [Color figure can be viewed in the online issue, which is available at wileyonlinelibrary.com.]

devoted that 48 h is the optimum time to ensure the remove of lignin and waxes.[24,26] The weight loss after alkali treatment is around 30%.

The polypropylene was modified with 8 wt % of SEBS-*g*-MA as a compatibilizer to be employed as a matrix in the woven doum composite and will be noted PP-FG1901X [Figure 1(a)]. The used coupling agent was chosen to optimize the surface adhesion between doum fibers and the polymer matrix.[27,28] The 8 wt % of SEBS-*g*-MA has been optimized in our previous work.[8,9,29] The compatibilized PP was extruded in a twin screw extruder (Leistritz Extrusionstechnik GMBH, Germany) at 125 rpm screw for the polymer and 40 rpm screw rotating for the compatibilizers.

The polymer granules were supplied in zone 0 using a mass control feeder, while addition of the coupling agent FG1901X was ensured by a mass control feeder that feeds a side-stuffer located in the fourth zone. The feed rate was of 1.2 kg/h. The temperature profile in the various zones along the extruder was 200, 200, 200, 200, 180, 180, 180, and 180°C at the die. The outlet side of the extruder was equipped with a die punt to adjust its opening and, therefore, to control the extruded film thickness. The adjustment of the punt opening along with the use of a calendaring system with a heating temperature of 100°C allowed obtaining films with 400 μm in thickness.[30,31]

Experimental Procedure

Composite Preparation. Hot press molding was done in an automatic press CARVER, under the following operating conditions: both upper and lower plates were heated to 200°C, after which a pressure of 4 MPa was applied to the composites. Composite films were molded in a rectangular shape (80 × 16 × 1) mm^3 as shown in Figure 4. Where the woven doum fibers were cut following the four characteristic directions dictated by the textile structure (0°, 15°, 30°, and 45°) to be impregnated in the polymer.

The samples for tensile and rheological tests were prepared from the composite films as shown in Figure 4(a,b).

Characterizations Techniques

ATR–FTIR Analysis. Fourier Transform-Infrared spectra were recorded on an ABB Bomem FTLA 2000-102 spectrometer

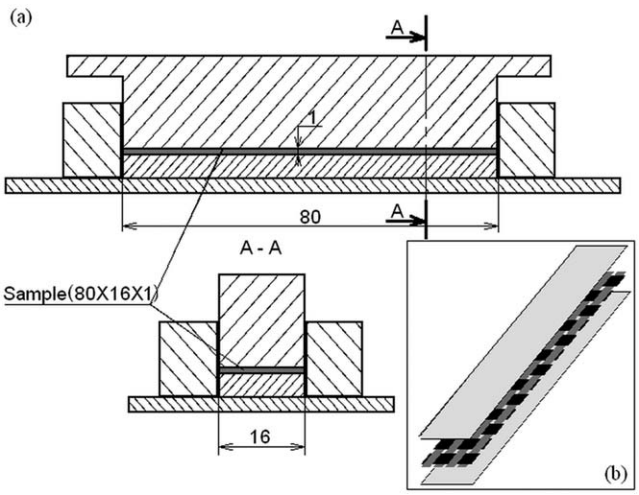

Figure 4. (a) Mold used to press sample; (b) the textile composite material.

Applied Polymer SCIENCE

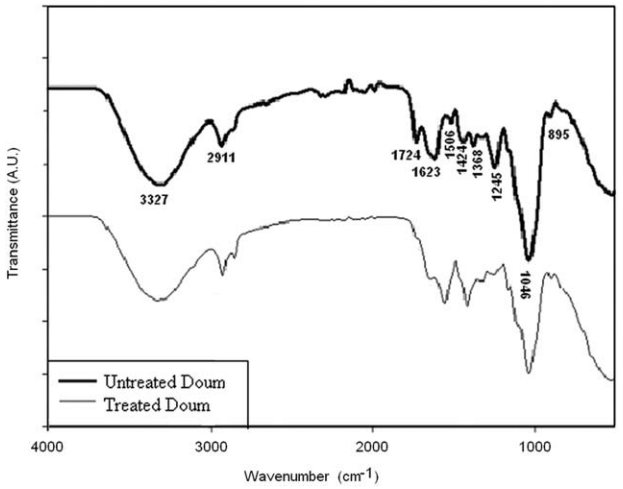

Figure 5. FTIR spectra of doum fibers (untreated, alkali treated) (4000–700 cm^{-1}).

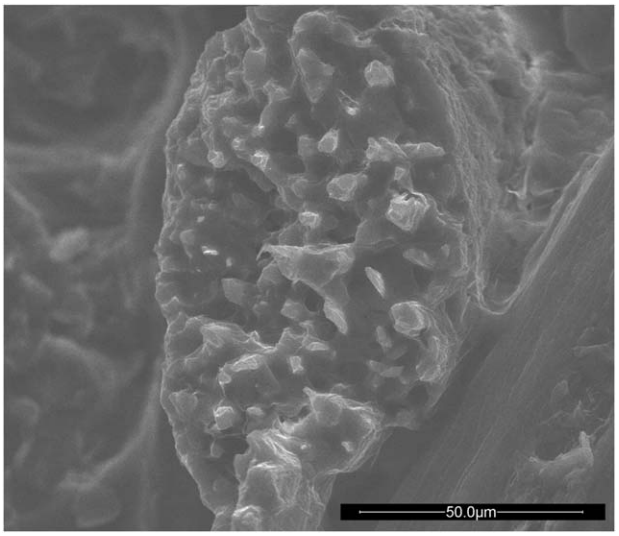

Figure 6. Morphology of doum fibers.

(using Specac Golden Gate). attenuated total reflectance (ATR) accessory with a resolution of 4 cm^{-1} was used.

Optical Microscope. The fiber morphology before and after alkali treatment was illustrated microscopically at ×10 and ×50 magnification on Leica microscope supported with Leica QWin V3 analysis software.

Scanning Electron Microscopy. Scanning electron microscopy (SEM) was used to illustrate the morphology of fibers, and evaluate the adhesion between fibers and the polymer matrix. To obtain clean and precise fracture faces, all composite samples were cryo-fractured.

Mechanical Testing

Tensile Testing. The tensile tests were performed on a universal testing machine INSTRON 8821S (Instron, USA) at a crosshead speed of 3 mm/min using a 5 kN load cell. The Young's modulus and tensile strength of the polypropylene composites were obtained according to the standard ISO 527-5.[32]

Dynamic Mechanical Thermal Analysis. The dynamic mechanical thermal properties were measured using a Rheometer Solid Analysis (RSA). The test samples were rectangular with 45 mm length, 7 mm width, and 1 mm thickness. The strain sweep test was performed at a frequency of 1 Hz. The frequency sweep test was carried from 0.015 to 15 Hz, with a strain rate controlled at 0.0001. The testing temperature was ranged from 30°C to 120°C, with a heating rate at 5 °C/min, and the set frequency was 1 Hz when the used strain was set at 0.0001.

Table I. IR Spectrum of Chemically Modified Doum

Wave number (cm^{-1})	Characteristic group
3327	—O—H[25]
2911	—C—H[26]
1724	C═O[25]
1623	—O—H[25]
1506	C═C[25]
1424	CH_2[25,27]
1368	In the -plane CH[25]
1245	C—C plus O—C plus C═O[25]
1046	C—C, C—OH, C—H[25]
895	COC, CCO, and CCH[25]

RESULTS AND DISCUSSION

Structural Characteristics of the Doum Fibers and its Composites

The FTIR spectra of untreated and alkali treated doum fibers are presented in Figure 5. This Figure shows that the spectra of the treated fibers have the same appearance to an untreated fiber. However, the intensity of the absorption band at around 1730 cm^{-1}, which corresponds to (C═O) stretching was found to depend on fiber modification. In alkali treated fibers curve, the intensity of C═O stretching disappeared due to the removal of non-cellulosic impurities, such as pectin and hemicellulose from the surface.[26] The infrared absorption peaks related to the main functional groups of the doum fibers are listed in Table I.

Scanning Electron Microscopy. The fiber is actually a bundle of hollow sub-fibers. The fibrillar-like structures of fibers can be observed in the fracture image SEM (Figure 6). And Figure 7 shows SEM micrographs of fractured surfaces of composite systems based on doum fibers. In the case of the composite without coupling agent, it can be observed an appearance of decohesion zones [Figure 7(a)]. This is a clear indication of the poor adhesion between lignocellulosic fibers and the matrix. On the other hand, Figure 7(b) shows a good adhesion between the fibers and the matrix with no noted decohesion, which is normal with the addition of coupling agent that improves the interfacial adhesion and thereafter enhances the mechanical properties.

Mechanical Properties

Tensile Properties. Generally, the mechanical properties of woven fabrics are governed by: woven architecture, yarn size, yarn spacing length, fiber orientation angle, fiber volume fraction.[18] Figure 8 illustrates the tensile measurements which were

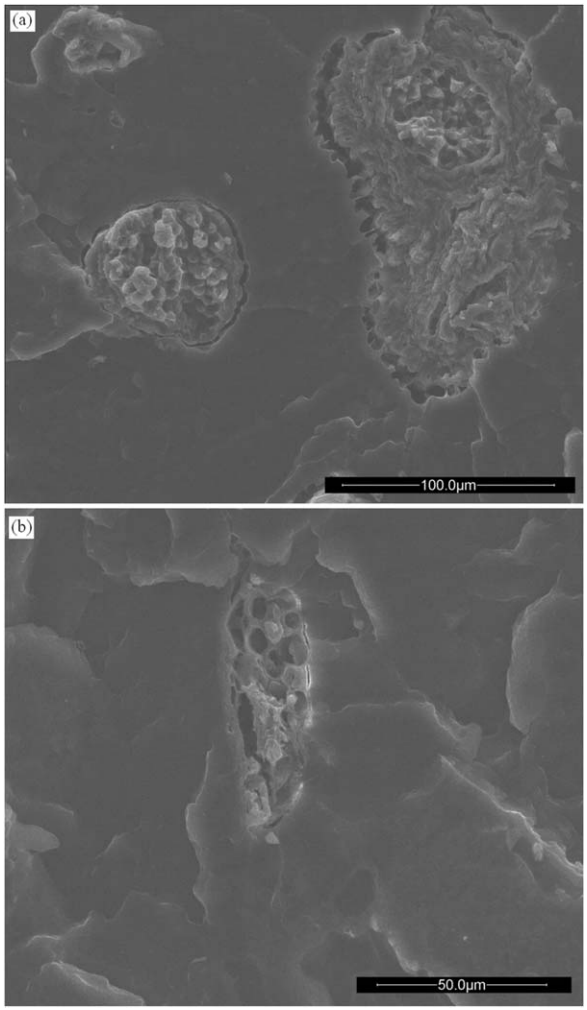

Figure 7. (a) Doum-PP without FG; (b) Doum-PP with FG.

carried out at a crosshead speed of 3 mm/min in an Instron tensile testing machine. The samples are molded in the characteristic directions dictated by the textile structure. These tests were conducted for five samples, from 0° to 45° (0°, 15°, 30°, and 45°) directions of the woven fibers. The young's modulus of the composites is evaluated by the slope of the curve in the linear region [Figure 8(a)]. Thus, the Young's modulus in 0°, 15°, 30°, and 45° direction were found at 2099, 1762, 1586, and 1563 MPa, respectively, which correspond to an increase of 103, 70, 53, and 51%, respectively compared to the neat PP. The illustrated values seems normal because in the longitudinal direction of fibers, i.e., (0°) the load is supported by the length of the unidirectional fibers[32] while out of this direction (15°, 30°, and 45°) the axial load forms an angle with yarns in both sides. Thus, the response in the first case (0°) behaves as a brittle solid while in the other case (15°, 30°, and 45°) the composite material retains the ductile behavior of the polymer [Figure 7(b)]. The results of tensile strength [Figure 8(c)] on the various directions were 24.3, 20.75, 15, 14.65MPa at 0°, 15°, 30°, and 45° direction, respectively. The mechanical tests demonstrate the highest mechanical properties in the principal fiber direction as supported in the literature.[33]

Modelization. The model used the same basic assumptions:

- The fibers and the matrix are linearly elastic, the matrix and the fibers are isotropic.
- The fibers are axisymmetric, identical in shape and size.
- The fibers and matrix are well bonded at their interface, and still remaining that way during deformation. Thus, the interface fiber/matrix debonding is not considered.

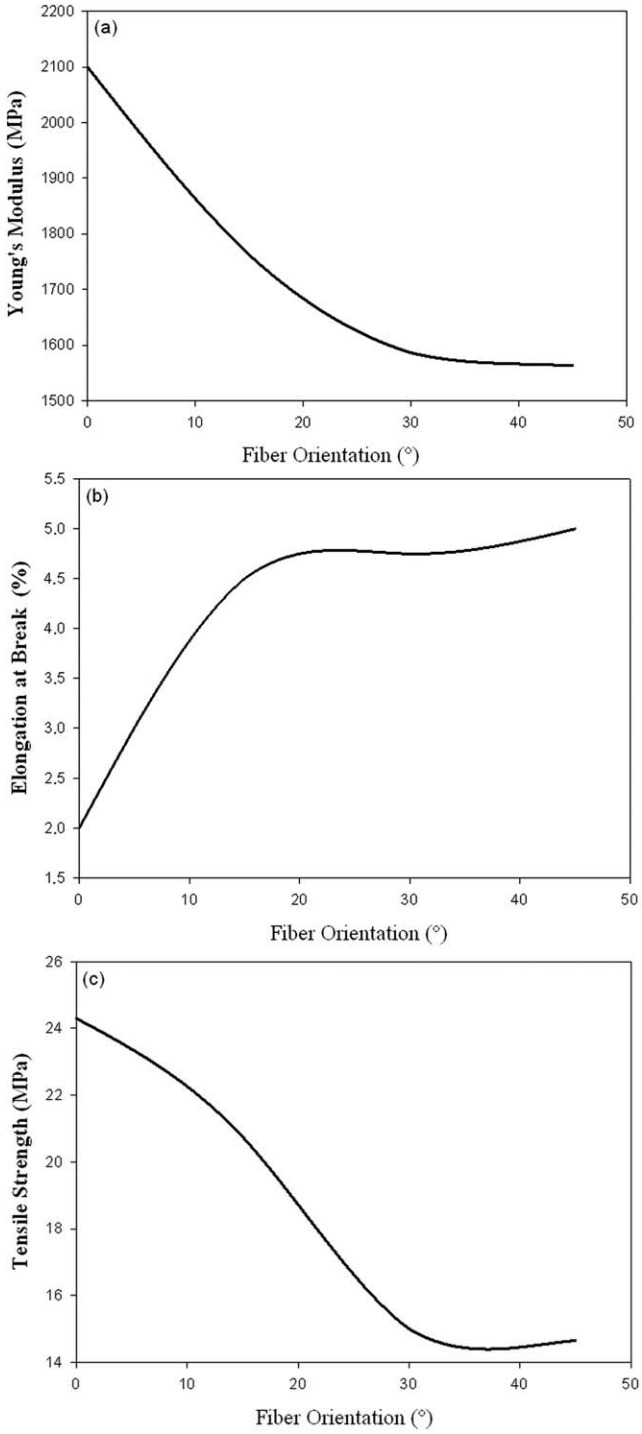

Figure 8. (a) Youngs modulus (MPa) vs. orientation; (b) elongation at break vs. orientation; (c) tensile Strength (MPa) vs. orientation.

Applied Polymer SCIENCE

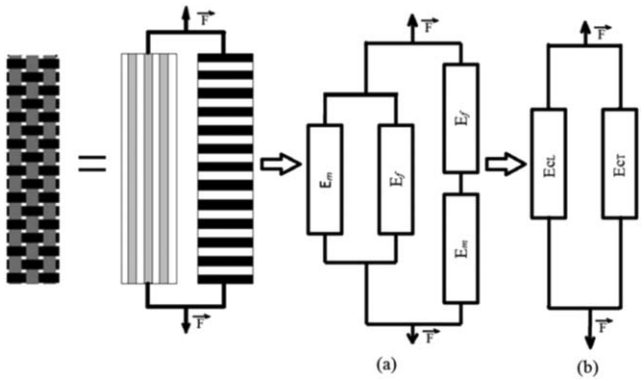

Figure 9. Use of Voigt and Reuss models.

This section will predict the young's modulus of different fiber direction in composite namely 0, 15, 30, and 45°. The predicted Young's modulus will be compared to the experimental ones.

Approach Description. Such methods have been developed to define the composites' stiffness as Voigt and Reuss models. We note that Voigt model corresponds to the assumption that fibers and the matrix are parallel to the applied stress, while Reuss model corresponds to the assumption that fibers and the matrix are normal to the applied stress. Hence, the drawing (Figure 9).

This combination of two models, Voigt and Reuss heckled us thinking about other directions namely 15, 30, and 45° hence Figure 10. Thus, in this article we will study the elastic behavior of woven composite material in two layers, expressed in a system of reference axis (L,T,T') and (x,y,T').

So to define the behavior of each layer at a θ angle, relative to the longitudinal direction "L," it is necessary to define the layer behavior in its principal base (L, T, T').

Cauchy generalized Hooke's law to three dimensional elastic volumes and stated that the six components of stress are linearly related to the six components of strain.

The stress–strain relationship written in tensor form, where the six components of stress and strain can be written using the summation convention [eq. (1)]:

$$\varepsilon_{ij} = S_{ijkl}\sigma_{kl} \tag{1}$$

where S_{ijkl} is the stiffness tensor, σ_{kl} the stress vector, and ε_{ij} the strain vector.

And so this is the form in which the strain is expressed in terms of the stress tensor in engineering [eq. (2)]:

$$\varepsilon_i = S_{ij}\sigma_j. \tag{2}$$

Moreover, we have assumed that the whole system is under a plane stress and is an orthotropic material. In that case stiffness tensor takes the following form:

$$S = \begin{pmatrix} S_{11} & S_{12} & 0 \\ S_{21} & S_{22} & 0 \\ 0 & 0 & S_{66} \end{pmatrix}_{L,\,T\,T'}$$

$$\text{where} \begin{cases} S_{11} = 1/E_L \\ S_{12} = -\nu_{LT}/E_L \\ S_{22} = 1/E_T \\ S_{66} = 1/G_{LT} \end{cases} \tag{3}$$

The E_L, and E_T are the parallel and normal Young's moduli, determined by Voigt and Reuss models. Where ν_{LT} and G_{LT} are Poisson's ratio and the shear modulus.

Hence, the Young's moduli E_L and E_T are expressed according to Voigt and Reuss models, respectively [eq. (4)]:

$$\begin{cases} E_L = V_f E_f + (1-V_f)E_m \\ E_T = \dfrac{E_f E_m}{V_f E_m + (1-V_f)E_f} \end{cases} \tag{4}$$

E_f is the fiber elastic modulus, E_m is the matrix elastic modulus, and V_f is the fiber volume fraction.

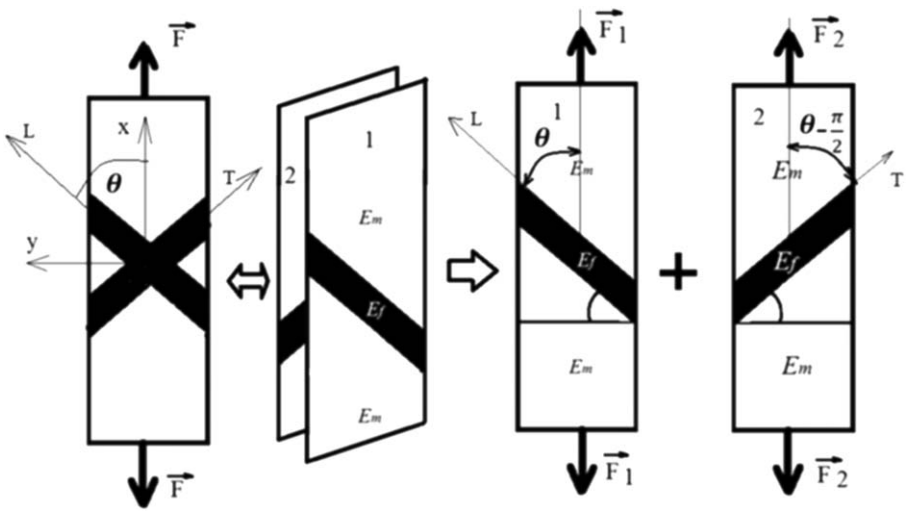

Figure 10. Approach modelization of Young modulus in different directions.

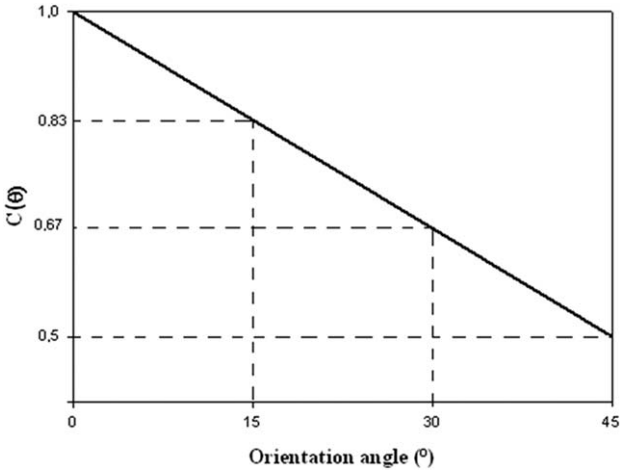

Figure 11. The linear interpolation of $C(\theta)$ in the range of 0 and 45°.

For more simplification v_{LT} is reduced to the Poisson's ratio of the matrix, where the Poisson's ratio of fibers is neglected. So the final Poisson's ratio could be expressed in the form [eq. (5)]:

$$v_{LT} = v_m(1 - V_f). \tag{5}$$

The shear modulus G_{LT} is in common form for isotropic material [eq. (6)]

$$G_{LT} = \frac{E_L}{2(v_{LT}+1)} \tag{6}$$

So, for each angle we will consider the rotation matrix defined in (L,T,T') base as

$$a = \begin{pmatrix} \cos\theta & -\sin\theta & 0 \\ \sin\theta & \cos\theta & 0 \\ 0 & 0 & 1 \end{pmatrix} \tag{7}$$

To find the different S'_{ijkl} stiffness tensor terms in (x, y, T') base, eq. (8) is used:

$$S'_{ijkl} = a_{im}\, a_{jn}\, a_{kp}\, a_{lq}\, S_{mnpq} \quad \text{(Einstein notation)}. \tag{8}$$

In this work, we need to define S'_{11} that is equal to $\frac{1}{E_x}$ and found from the eq. (8) at the form:

$$S'_{11} = S_{11}\cos^4\theta + S_{22}\sin^4\theta + (2S_{12} + S_{66})\sin^2\theta\cos^2\theta \tag{9}$$

From eqs. (3) and (9) the S'_{11} will be expressed by eq. (10) as:

$$S'_{11} = \frac{\cos^4\theta}{E_L} + \frac{\sin^4\theta}{E_T} + \left(2\frac{v_{LT}}{E_L} + \frac{1}{G_{LT}}\right)\sin^2\theta\cos^2\theta \tag{10}$$

For the assembly of the two layers (at θ and$90° - \theta$ fiber directions), lets introduce one coefficient $C(\theta)$ which represents the contribution of each layer. The values of $C(\theta)$ are deducted from a linear interpolation in the range of 0–45° (Figure 11).

The Young's modulus for each direction can be expressed by the eq. (11):

$$E_L(\theta) = C(\theta)E_{x_1} + (1 - C(\theta))E_{x_2} \tag{11}$$

The elastic modulus of untreated and treated doum fibers was measured by experimental approach, using the Rheometer Solid Analysis (Monofilament), using a rectangular tension/compression geometry. The elastic modulus of untreated doum fiber is 2.65 GPa, however, after chemical treatments the elastic modulus of the treated doum is 6 GPa.

Table II. summarized of the Young's Modulus for Each Direction

Angle (°)	$E_x(\theta)$ (MPa)	$C(\theta)$	$E_L(\theta)$ (MPa)	E_{exp} (MPa)
0	2593	1	2593	2100
15	2585	0.83	2398	1759
75	1486			
30	2461	0.67	2226	1586
60	1751			
45	2136	0.5	2136	1565

Application. From the voigt and Reuss models and eqs. (4)–(6) we find

E_L = 2593 MPa
E_T = 1397.08 MPa
v_{LT} = 0.244
G_{LT} = 926.07 MPa
where

E_f = 6000 MPa; E_m = 1034 MPa; V_f = 0.314; v_m = 0.4.

And Table II summarizes the Young's modulus for each direction.

The observed difference in the results (predicted Young's modulus and experimental one) are mainly due to the assumption taken before, when in the reality the adhesion isn't perfect and the woven technique leads to corrugated fiber which reduce their stiffness.

Figure 12 shows the introduction of a shrinkage parameter in the Young's modulus predicted form compared to the experimental modulus and to the previously measured modulus $E_L(\theta)$. The new measured Young's modulus is calculated on taking on account the Young's modulus of the corrugated fiber [eq. (12)]:

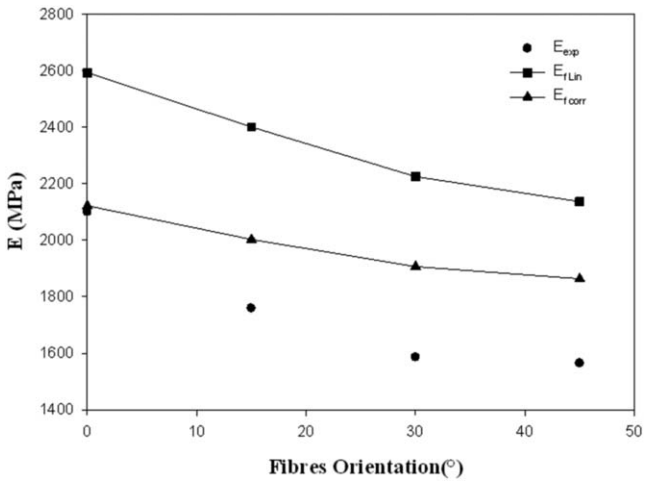

Figure 12. The evolution of Young Modulus vs. fiber orientation.

Applied Polymer SCIENCE

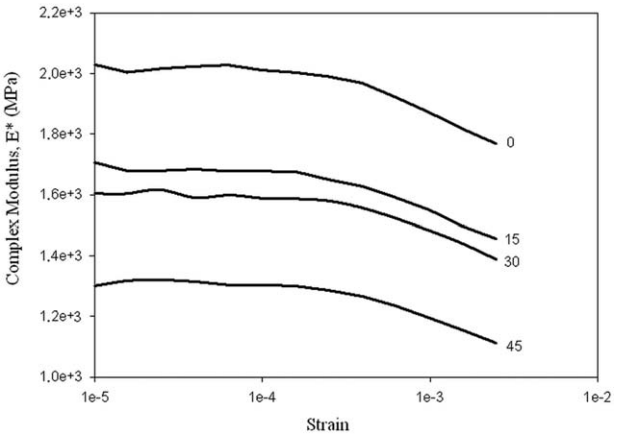

Figure 13. Dynamic modulus (E^*) vs. strain.

$$E_{f_{corr}} = yE_{f_{lin}} \quad (12)$$

where $E_{f.corr}$, $E_{f.lin}$ are the Young's moduli of corrugated fiber, and the linear fibers, respectively. The y is the correlated coefficient to characterize undulation ($y = 0.75$).

The noted difference between the new $E_L(\theta)$ and experimental results is attributed to the surface adhesion between woven fibers and the matrix that is not perfect.

Dynamic Mechanical Thermal Analysis. Dynamic mechanical analysis methods have been widely employed for investigating the structures and viscoelastic behavior of polymeric materials, also to determine their relevant stiffness and damping characteristics for various applications.[34] The dynamic properties of polymeric materials are of considerable practical significance when determined over a range of temperature, strain, and frequencies.[34]

Depending on the used coupling agent and woven fibers direction, both complex modulus (E^*) and loss factor (tan δ) are affected as depicted in the results. The complex modulus (E^*) is expressed using eq. (13) and tan δ by the eq. (14)[35]:

$$E^*(\omega) = E'(\omega) + iE''(\omega) \quad (13)$$

$$\text{Tan } \delta = E''(\omega)/E'(\omega). \quad (14)$$

Therefore, the storage modulus (E') and the loss modulus (E'') are defined by eqs. (15) and (16).

$$E' = (\sigma_0/\varepsilon_0) \ cos \ \delta. \quad (15)$$

$$E'\prime = (\sigma_0/\varepsilon_0) \ sin \ \delta. \quad (16)$$

A strain sweep test was performed on the woven fiber composites in order to establish the linear viscoelastic regime and to characterize the strain dependent viscoelastic properties of the samples.

The determination of the linear range is performed by observing the variation of the complex modulus (E^*) with an increase of the deformation. Figure 13 shows the effect of woven fibers directions on complex modulus (E^*) at 1 Hz frequency. It is seen that the complex modulus (E^*) decreases with increasing direction angle from 0° to 45°. This was probably because the fibers in the unidirectional woven fabrics were stressed by the tensions applied during spinning and weaving, resulting in a higher initial modulus of the final composites[36] compared to the fibers with orientation, because the load forms an angle with both sides. These results are confirmed and explained by the tensile test.

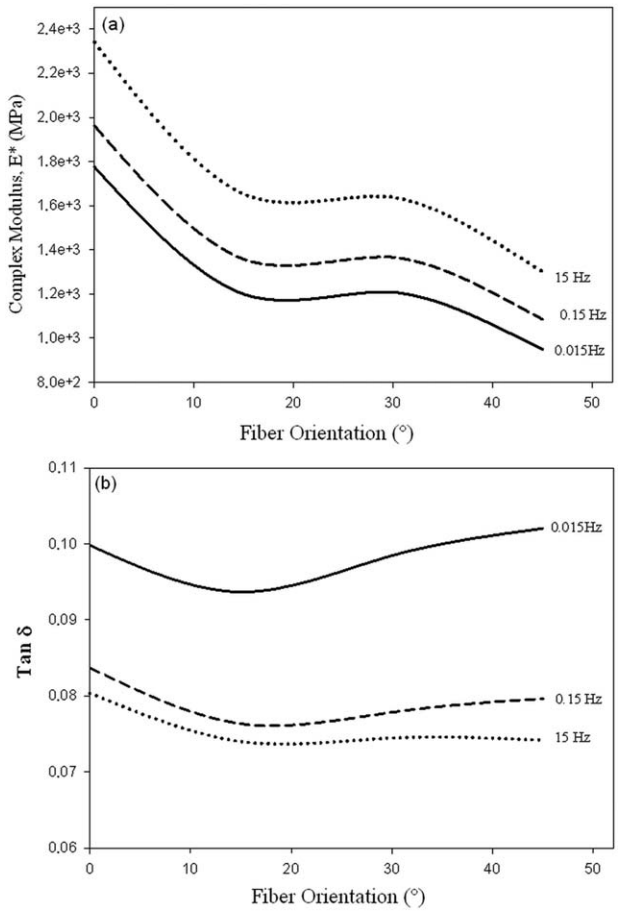

Figure 14. (a) Dynamic modulus (E^*) vs. frequency; (b) tan δ vs. frequency.

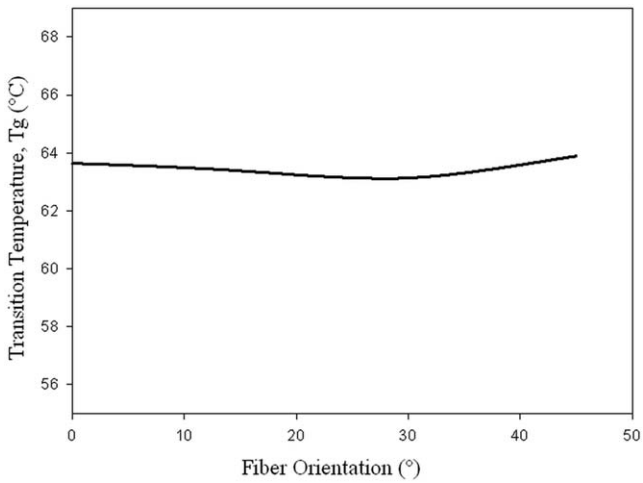

Figure 15. Glass temperature evolution vs. woven fiber orientation.

Dynamic frequency sweep tests were performed at a range of frequencies from 0.015 to 15 Hz, afterward using strain amplitude of 0.0001. The evolutions of the complex modulus and mechanical loss factor, for the woven fibers direction (0°, 15°, 30°, and 45°), are illustrated in Figure 14. It can clearly be seen an evolution in complex modulus [Figure 14(a)] and a progressive decrease in loss factor (tan δ) [Figure 14(b)] from the low to the highest frequency. At high frequencies, the molecules have no time to undergo permanent deformation, the relaxation time of the molecular chains is higher than the time of solicitation, and such that the material exhibits an elastic behavior.[37] However, when the frequencies are lower the molecules get time to slip past one another and flow occurs. This viscous behavior causes decrease in damping factor values, which is indicated by an increase in storage modulus (E'), therefore an increase in E^* values, with increase in frequencies.[37]

Also, Figure 14(a) shows the variation of complex modulus (E^*) with varying stress direction. And it is observed that the modulus decreased steadily from 0° to 45° woven fiber direction. The composite at 0° shows a higher complex modulus than the other ones (15°, 30°, and 45°) which can be due to the rigidity of the longitudinal fiber when load was applied.[5] It was also observed in Figure 13(b) that the loss factor is nearly remaining constant with varying the stress direction. The viscous behavior of the material causes an increase on the storage modulus (E'') and a decrease in the loss modulus value (E').[37] Therefore, the loss factor (tan δ) remains constant and is not affected by stress direction. The impact properties can be deduced from the dynamic mechanical analysis (tan δ), which characterize the viscous part versus elastic part and compared to neat PP, these properties were not affected, which can be explained by the rubber character of the coupling agent.

Glass Transition. The temperature at which the (tan δ) peak occurs is commonly known as the glass transition temperature (T_g).The variation of T_g as a function of stress directions is shown in Figure 15. T_g was evaluated from the peaks of tan δ vs. temperature. It was observed in Figure 15 that the T_g is nearly constant (about 63°C) with respect to the variation of stress direction (from 0° to 45°). It is well known that the glass transition temperature is associated with conformational crank shafting movements of the main chain.[35,38] Therefore, the direction of woven's fibers has no effect on the T_g (isotropy of T_g) and so on the thermal stability of composites.

CONCLUSION

In this study, a textile structure was manufactured using a homemade system and doum long fibers to be impregnate with polypropylene compatibilized with SEBS-*g*-MA to perform its mechanical properties. The used samples were made according to four main directions 0°, 15°, 30°, and 45° to see the effect of fiber orientation in the analyzed properties. Thus, the tensile properties were largely higher in the orthogonal direction i.e. (0°) than the remaining (15°, 30°, and 45°) directed sample, and because of the reinforcement, the tensile properties of all woven direction are higher than the neat PP. Moreover, the predicted Young's moduli in each fibers directions are found near to the experiment with an error due to common assumption that are not always true.

Also, a dynamic mechanical thermal analysis (DMTA) analysis were carried out and it was observed that as stress direction increases from 0° to 45°, the values of E^*, the dynamic modulus decrease whereas tan δ, the loss factor remain constant. The DMTA tests had illustrated good viscoelastic properties at longitudinal direction (0°) and lower properties when increasing to 45° directed sample.

ACKNOWLEDGMENTS

This work was supported by MAScIR; Moroccan Foundation for Advanced Science, Innovation and Research and Hassan II Academy of Science and Technology.

REFERENCES

1. Bledzki, A. K.; Gassan, J. *Prog. Polym. Sci.* **1999**, *24*, 274.
2. Wambua, P.; Ivens, J.; Verpoest, I. *Compos. Sci. Technol.* **2003**, *63*, 1259.
3. Abdelmouleh, M.; Boufi, S.; Belgacem, M. N.; Dufresne, A. *Compos. Sci. Technol.* **2007**, *67*, 1627.
4. Arrakhiz, F. Z.; Elachaby, M.; Bouhfid, R.; Vaudreuil, S.; Essassi, M.; Qaiss, A. *Mater. Design* **2012**, *35*, 318.
5. Arrakhiz, F. Z.; El Achaby, M.; Kakou, C. A.; Vaudreuil, S.; Benmoussa, K.; Bouhfid, R.; Fassi Fehri, O.; Qaiss, A. *Mater. Design* **2012**, *37*, 379.
6. Torres, F. G.; Cubillas, M. L. *Polym. Test.* **2005**, *24*, 694.
7. Madsen, B.; Hoffmeyer, P.; Lilholt, H. *Compos. Part A* **2007**, *38*, 2204.
8. Essabir, H.; Nekhlaoui, S.; Malha, M.; Bensalah, M. O.; Arrakhiz, F. Z.; Qaiss, A.; Bouhfid, R. *Mater. Design* **2013**, *51*, 225.
9. Essabir, H.; Hilali, E.; Elgharad, A.; El Minor, H.; Imad, A.; Elamraoui, A.; Al Gaoudi, O. *Mater. Design* **2013**, *49*, 442.
10. Harish, S.; Peter Michael, D.; Bensely, A.; Mohan Lal, D.; Rajadurai, A. *Mater. Charact.* **2009**, *60*, 44.
11. Xie, Y.; Hill, C. A. S.; Xiao, Z.; Militz, H.; Mai, C. *Compos. Part A* **2010**, *41*, 806.
12. Mizanur Rahman, M.; Khan, M. A. *Compos. Sci. Technol.* **2007**, *67*, 2369.
13. Franco-Marquès, E.; Méndez, J. A.; Pèlach, M. A.; Vilaseca, F.; Bayer, J.; Mutjé, P. *Chem. Eng. J.* **2011**, *166*, 1170.
14. Ismail, H.; Shuhelmy, S.; Edyham, M. R. *Eur. Polym. J.* **2002**, *38*, 39.
15. Bengtsson, M.; Gatenholm, P.; Oksman, K. *Compos. Sci. Technol.* **2005**, *65*, 1468.
16. John, M. J.; Anandjiwala, R. D. *Compos. Part A* **2009**, *40*, 442.
17. Setz, S.; Stricker, F.; Kressler, J.; Duscher, T.; Mulhaupt, P. J. *Appl. Polym. Sci.* **1996**, *59*, 1117.
18. Tan, P.; Tong, L.; Steven, G. P. *Compos. Part A* **1997**, *28*, 903.

19. Karkkainen, R. L.; Sankar, B. V.; Tzeng, J. T. *Compos. Part B* **2007**, *38*, 924.
20. Mouritz, A. P.; Bannister, M. K.; Falzon, P. J.; Leong, K. H. *Compos. Part A* **1999**, *30*, 1445.
21. Tarnopol'skii, Y. M.; Kulakov, V. L.; Aranautov, A. K. *Comput. Struct.* **2000**, *76*, 115.
22. Nekhlaoui, S.; Qaiss, A.; Bensalah, M. O.; Lekhder, A. *Adv. Theor. Appl. Mech.* **2010**, *3*, 253.
23. Essabir, H.; Elkhaoulani, A.; Benmoussa, K.; Bouhfid, R.; Arrakhiz, F. Z.; Qaiss, A. *Mater. Design* **2013**, *51*, 780.
24. Le Troedec, M.; Sedan, D.; Peyratout, C.; Bonnet, J. P.; Smith, A.; Guinebretiere, R.; Gloaguen, V.; Krausz, P. *Compos. Part A* **2008**, *39*, 514.
25. Ku, H.; Wang, H.; Pattarachaiyakoop, N.; Trada, M. *Compos. Part B* **2011**, *42*, 856.
26. Rachini, A.; Peyratout, C.; Rossignol, S.; Max, E.; Kaftan, O.; Fery, A.; Smith, A. J. *Colloid Interface Sci.* **2011**,*356*, 303.
27. Pracella, M.; Chionna, D.; Anguillesi, I.; Kulinski, Z.; Piorkowska, E. *Compos. Sci. Technol.* **2006**, *66*, 2218.
28. Arrakhiz, F. Z.; El Achaby, M.; Benmoussa, K.; Bouhfid, R.; Essassi, E. M.; Qaiss, A. *Mater. Design* **2012**, *40*, 528.
29. Elkhaoulani, A.; Arrakhiz, F. Z.; Benmoussa, K.; Bouhfid, R.; Qaiss, A. *Mater. Design* **2013**, *49*, 203.
30. Qaiss, A.; Bousmina, M. *Polym. Eng. Sci.* **2011**, *51*, 1347.
31. Qaiss, A.; Saidi, H.; Fassi-Fehri, O.; Bousmina, M. J. *Appl. Polym. Sci.* **2012**, *123*, 3425.
32. ISO 527–5: 2009. Plastics—Determination of Tensile Properties—Part 5: Test Conditions for Unidirectional Fibre-Reinforced Plastic Composites; BSI Group: London, **2009**.
33. Miao M.; Shan, M. *Compos. Sci. Technol.* **2011**, *71*, 1713.
34. Goertzen, W. K.; Kessler, M. R. *Compos. Part B.* **2007**, *38*, 1.
35. Montazeri, A.; Pourshamsian, K.; Riazian, M. *Mater. Design.* **2012**, *36*, 408.
36. Bourmaud, A.; Baley, C. *Polym. Degrad. Stab.* **2009**, *94*, 297.
37. Geethamma, V. G.; Kalaprasad, G.; Groeninckx, G.; Thomas, S. *Compos. Part A* **2005**, *36*, 1499.
38. Pothan, L. A.; Oommen, Z.; Thomas, S. *Compos. Sci. Technol.* **2003**, *63*, 283.